Contents lists available at http://qu.edu.iq

Al-Qadisiyah Journal for Engineering Sciences

Journal homepage: https://qjes.qu.edu.iq

Experimental investigation of heat transfer in a cavity filled with (50% CuO-50% Al_2O_3)/Water with hybrid nanofluid attached to a vertically heated wall partially integrated with PCM

***Muqdad Al-Maliki and Khaled Al-Farhany* ***

Department of Mechanical Engineering, College of Engineering, University of Al-Qadisiyah, Al-Qadisiyah, 58001, Iraq

ARTICLE INFO

Article history:
Received 03 September 2022
Received in revised form 08 October 2022
Accepted 07 February 2023

Keywords:
(50% CuO-50% Al2O3)/Water
Hybrid nanofluid
Natural convection
PCM
Rectangular Cavity

ABSTRACT

An empirical evaluation of free convective heat transmission was conducted in a rectangular enclosure containing a hybrid nanofluid of (50% CuO-50% Al_2O_3)/water linked to a PCM-containing wall. The enclosure's left and right surfaces were kept at constant warm and cold temperatures, whereas the remaining surfaces were assumed to be isolated. The left side was filled partially with PCM. Several variables were examined, such as the hot-side temperature differential (ΔT =10, 15,20 ◦C) and the hybrid nanofluid concentration (Φ=0.03,0.05,0.07)%. The findings show that the rate of heat transmission through natural convection rises as the concentration of nanomaterials rises. Due to its great absorbability and heat storage capacity, PCM was also shown to have the potential to lower the hot side temperature by up to 15.5%. The Nusselt number rises over time as the left cavity is filled partially with PCM. When added hybrid nanofluid is, PCM's heat-storage efficiency and, by extension, its ability to cool the hot side is greatly improved.

1. Introduction

Many technical applications rely on an enclosure's convective heat transmission properties., such as solar energy and electronic cooling. Natural heat transfer in cavities is something that has been studied experimentally and theoretically for years, with a focus on active and passive strategies to increase efficiency. To improve the working fluid's thermal conductivity, nanoparticles have been introduced to the base fluid by numerous writers. [1-5]. Other scientists looked at hybrid nanofluids and their impact on heat transmission [6-11]. Today, the cost of energy and its impact on the environment are the most important factors to consider when developing thermal engineering systems. Academics' interest in thermal energy storage and associated technologies has therefore recently increased. There is a large amount of information about the application of PCM in thermal engineering may be found in [12-19].

Shili et al. [20] conducted experimental and numerical studies of the heating plate and analysis of the effects of liquid choice on the PCM. Siloil and Water are utilized in closeness to phase change materials (synthetic paraffin). To generate heat, a rectangular enclosure was placed between two parallel walls. Because of the surrounding liquid, PCM is insulated from the hot plate. According to the findings, Keeping PCM to a minimum in the liquid enhances thermal conductivity and heat transfer at a warm surface. The copper's temperature sheet drops by around 20% when Water is used to surround the PCM.

* *Corresponding author.*
E-mail address: khaled.alfarhany@qu.edu.iq (Khaled Al-Farhany)

https://doi.org/10.30772/qjes.v16i1.912

Kean et al. [21] performed a numerical study of the fusion of PCM composite with nanomaterials within a square enclosure and its impact on natural convective heat transfer. Two cases have been conducted; the first case considers the vertical wall as a hot surface, whereas the second case, the horizontal base wall, includes one of the hot walls. The temperature on the left surface is always hot, while the temperature on the opposite wall is always cold. Alumina, copper oxide, nanoparticles are employed in different concentrations of 0, 2, and 5 %. In this simulation, the enthalpy porosity method is used to melt a NEPCM in a square enclosure, while the finite volume method is used to solve the dominating equations. The result shows that a low nanoparticle concentration increased heat transfer rate. The heating from the enclosure's sidewalls causes melt quicker than heating from below.

Sivashankar et al. [22] used PCM and graphene nanoplatelets to explore heat transmission in concentrated photovoltaic (CPV) cells loaded (GNP). The efficiency of a pure PCM-based CPV cell is explored, and the outcomes are comparable to those of a CPV cell with nano-augmented PCM (n-PCM). The heat from the CPV is transferred using an aluminum heat sink with longitudinal fins. The concentrations of GNP (0.1% - 0.5%). The results show that the heat conductivity of different volume concentrations for nPCM is measured and compared to the thermal conductivity of pure PCM. For a 0.5% volume concentration, the highest increase of thermal conductivity in liquid and solid stages was found to be 75% and 22%, respectively.

Ebadi et al. [23] conducted energy storage and heat transfer specifics of a Cylindrical Thermal Energy Storage (C-TES) device using bio-based nanoPCM. The parameters are used in the survey the Rayleigh number ($10^6 \leq Ra \leq 10^8$) and the hybrid nanofluid's solid volume fraction ($0 \leq \Phi \leq 0.05$). The bottom of the C-TES system is isolated, and the lateral walls and top are isothermally heated. The results reveal that the distinction in stored energy with the Rayleigh number is less at the meeting's start; however, as the melting advances to the convection-dominated regime, the discrepancy grows higher due to augmented melting at the more significant Rayleigh number.

Abdelrazik et al. [24] discussed the electrical and thermal efficiency of a hybrid PV/PCM module and PV/thermal system during the application of a layer of (nanoPCM). The nanoparticles loading of the PW/GNP nanoPCM ($0 \leq \Phi \leq 20\%$). The upper partition of the cavity is exposed to a hot temperature representing the temperature of the photovoltaic cell. The lower wall is a cold temperature representing the temperature of the cooler. The results show that in most cases, different loadings of GNP in Paraffin wax PCM improve the cooling and electrical efficiency of the PV panel. As the percentage of nanoparticles volume fraction increases, the PV panel temperature decreases, and the electrical effectiveness increases. Utilization phase change materials and Al_2O_3 nanoparticles,

Nada et al. [25] investigated temperature control and efficacy increase of PV-integrated building systems. Using pure PCM, two distinct (PV-PCM) modules were created. And the other using PCM with adding nanoparticles. The intensity of solar radiation, and wind speed were the parameters utilized. The outcomes demonstrate that adding Al_2O_3 nanoparticles to the PCM improves the heating effectiveness and temperature management of the combined components. Using PV in conjunction with pure PCM and enhanced PCM with nanoparticles may reduce module temperature by 8.1 and 10.6 °C, respectively, whereas increasing effectiveness by 5.7 and 13.2%. Chavan et al. [26] surveyed numerical investigation of the melting procedure in a rectangular chamber is free convection. A compound phase The foundation material is a composite phase transition substance (Paraffin wax 98%) containing copper nanoparticles (2 %) added. The enclosure on one side is heated, isothermal on the other, and each side is thermally insulated. The outcomes demonstrate that the shallow enclosure had a faster charging/discharge rate than the huge enclosure (up to 10 % less).

This study investigated experimentally the effect of partially filled PCM on the nanofluid's surface rectangular enclosure filled with hybrid nanofluid. Deferent volume fractions and temperature differences were used as parameter studies.

2. The Experimental Work

2.1. Experimental Rig

The primary components of the experimental environment are outlined below. The experimental plan is shown in **Fig. 1**, and the equipment used in the experiment is shown in **Fig. 2**. The heating system include a controller, a heater, and a DC energy supply. while the temperature-controlled water bath is used for the cooling unit. A thermal camera and data logger were used to measure the temperature distribution in the cavities.

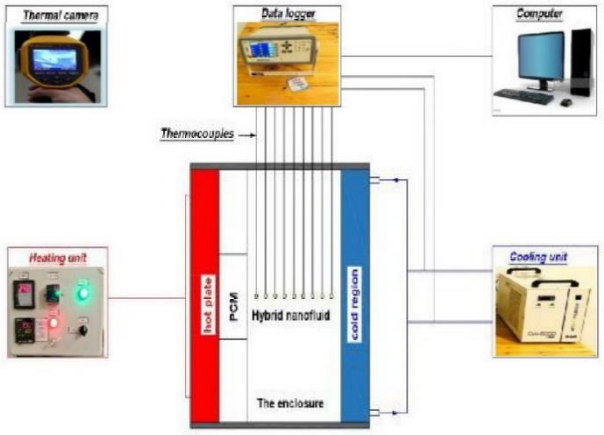

Figure 1. Schematic of the experimental apparatus.

Figure 2. Experimental equipment. (1) Sensitive equilibrium (2) A mechanical stirrer, (3) an ultrasonic wave generator, (4) a FLIR E30bx Thermal Camera, (5) a data logger, a PC, and a test section are all included.

2.2. Test Section

The test platform is shown in **Fig. 3** as two rectangular Perspex glass chambers with a thickness of 0.5 cm. The left enclosure is 20 cm high and 3 cm wide and separated into three evenly spaced horizontal grooves loaded with PCM. The left cavity is adhesive to the hot surface and is produced from an aluminum plate warmed up by a temperature-controlled electric heater. The right side is sticky to the cold surface, which is 20 cm high and 10 cm wide. It is designed to function as a heat exchanger made of aluminum plates to adjust the temperature by circulating water through it and is filled with a hybrid nanofluid. To detect temperatures at the walls, three thermocouples were installed in each right and left wall, and also, 35 thermocouples were installed in the cavity's center to measure temperature dispersion throughout the casing, as illustrated in **Fig. 4**.

Table 1. Perspex glass properties [27]

Physical properties	*Density*	*Thermal expansion coefficient*
Perspex glass	(1.17-1.2) (g/cm^3)	(5-10)×10^5 (K^{-1})

Figure 3. Enclosure assembly.

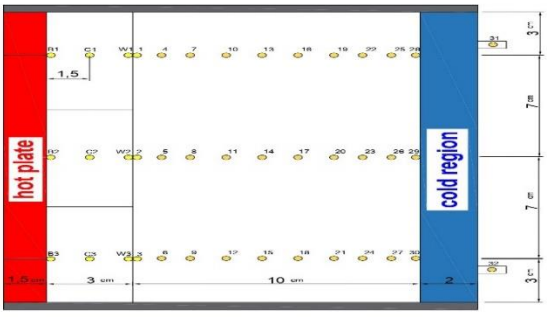

Figure 4. Thermocouple Position Within the Cavities.

2.3. PCM formulation and characterization

PCM is defined as any material that can be used to store or release thermal energy while its phase changes. Melting is connected with heat absorption, while solidification is related to heat release. In this study, paraffin wax, also known as RT-42, was employed as a latent heat material. It was locally purchased. As illustrated in **Fig. 5**, it had the trademark AL-HADDER LAICA. Paraffin melts at a temperature of 43 °C and solidifies at 38 °C. This material has a latent heat of 147 kJ/kg. The thermal conductivity of paraffin wax is 0.2 W/m.K. Table 2 contains further thermophysical parameters of the paraffin utilized, [**31**]. Additionally, two kilograms of paraffin were used in this study shown in Figure 5.

Figure 5. The PCM utilized in this work.

Table 2. Physical characteristics of the paraffin Wax RT42 [28]

T solidus	38 °C
T liquidus	43 °C
Latent heat of melting	174 kJ/kg
Density	800 kg/m³ (solid) 760 kg/m³ (liquid)
Thermal expansion coefficient	0.00081/°k
Specific heat capacity	2 kJ/kg. K
Thermal conductivity	0.2 W/m.K

2.4. Preparation of Hybrid nanofluid

Nanoparticles have been added to the basic fluid to improve the thermal-physical characteristics expectantly. A hybrid nanofluid (50% CuO-50% Al_2O_3)/water has been produced with 0.03, 0.05, and 0.07 % varied volume concentrations. This requires several processes, which are described in the sections below:

1- Calculate the mass of CuO and Al_2O_3 using **Eq. 1** [29]**.**

$$\Phi\% = \frac{(\mathbf{W}/\boldsymbol{\rho})_{CuO}+(\mathbf{W}/\boldsymbol{\rho})_{Al_2O_3}}{(\mathbf{W}/\boldsymbol{\rho})_{CuO}+(\mathbf{W}/\boldsymbol{\rho})_{Al_2O_3}+(\mathbf{W}/\boldsymbol{\rho})_{water}} \quad (1)$$

2- In **Table 3,** can be seen the necessary mass for each type of hybrid nanofluid.
3- An ultrasonic wave device has been employed for 4 hours to achieve an effective and uniform dispersion of nanoparticles and a stable mixing
4- SDS (1% wt) was added to the CuO-Al2O3/water hybrid nanofluid to enhance stability. [30].
5- Use the mechanical stirrer for 1 hour to achieve mixture homogeneity and get the desired nanoparticle volume fraction.

Table 3. Mass of nanoparticles for each concentration.

The concentration of Nanoparticles %	**Mixing rate**	**Mass of CuO (g)**	**Mass of Al_2O_3 (g)**
0.03	30%CuO+70%Al_2O_3	1.7	4
	40%CuO+60%Al_2O_3	2.4	3.6
	50%CuO+50%Al_2O_3	3.15	3.15
Total weight		7.25	10.75

2.5. Calculating the Hybrid nanofluid's thermophysical properties

The thermophysical characteristics of hybrid nanofluids are crucial in heat transport. It is possible to calculate the nanofluid's density, thermal conductivity, and effective viscosity using **Eqs. 2 to 6** [31].

$$\rho_{hnf} = \Phi_{Cuo}.\rho_{Cuo} + \Phi_{Al2o3}.\rho_{Al2o3} + \left(1 - \Phi_{hnf}\right)\rho_{bf} \quad (2)$$

The heat capacitance of hybrid nanofluid (ρCp) h_{nf} is:

$$\rho_{hnf}.Cp_{hnf} = \Phi_{Cuo}.\rho_{Cuo}.Cp_{Cuo} + \Phi_{Al2O3}.\rho_{Al2O3}.Cp_{Al2O3} + (1 - \Phi_{hnf}).\rho_{bf}.Cp_{bf} \quad (3)$$

The buoyancy coefficient of hybrid nanofluid (ρβ)hnf can be determined as:

$$(\rho\beta)_{hnf} = \Phi_{Cuo}.\rho_{Cuo}.\beta_{Cuo} + \Phi_{Al2O3}.\rho_{Al2O3}.\beta_{Al2O3} + (1 - \varphi_{hnf}).\rho_{bf}.\beta_{bf} \quad (4)$$

The Brinkman and Maxwell model is used to calculate the dynamic viscosity ratio of a hybrid nanofluid given by **[32]** as follows:

$$\frac{\mu_{hnf}}{\mu_{bf}} = \frac{1}{(1-(\Phi_{Cuo}+\Phi_{Al2O3})^{2.5}} \quad (5)$$

Thermal conductivity is calculated using (Maxwell correlation)**[32]:**

$$\frac{k_{hnf}}{k_{bf}} = \frac{\left(\frac{(\varphi_{Cuo}.k_{cuo}+\varphi_{Al2O3}.k_{Al2o3})}{\emptyset_{hnf}}+2kbf+2(\varphi_{Cuo}.k_{cuo}+\varphi_{Al2O3}.k_{Al2o3})-2\emptyset_{hnf}.k_{bf}\right)}{\frac{(\varphi_{Cuo}.k_{cuo}+\varphi_{Al2O3}.k_{Al2o3})}{\emptyset_{hnf}}+2k_{bf}-2(\varphi_{Cuo}.k_{cuo}+\varphi_{Al2O3}.k_{Al2o3})+\emptyset_{hnf}.k_{bf}} \quad (6)$$

2.6. Experimental procedure and calculations

In this study, different parameters have been used, including; the volume fraction of nanoparticles and the variation in temperature between the warm and chill surface, using PCM in one part of the left hot wall. These tests are all completed on schedule and at three separate times (t=15, 30, and 60 minutes). Thermophysical characteristics of the (50% CuO-50% Al_2O_3)/nanofluid were first obtained at the (0.03 %, 0.05 %, and 0.07 %) nanoparticle concentrations. Second, consider the temperature difference between cold and warm surfaces set at (10, 15, and 20 ◦C). Finally, after collecting all temperature readings within the cavity and capturing thermal photos with the Fluke Ti300+ Thermal Imaging Camera for each temperature difference, concentration, and duration.

2.7. Device initialization

Before doing any testing, it is critical to evaluate the device's initial processes:

1. The cavity's left side that contacts a hot wall is filled partially with a PCM, and the right side of the cavity that contacts a cold wall is loaded with a hybrid nanofluid.
2. A water bath was employed to maintain a consistent temperature at the cold wall, while the hot wall was supplied with heaters, a thermostat, and an appropriate AC power supply.
3. AT45xx Multi-Channel Temperature Meter was utilized to record temperatures over time. When the temperature differential is smaller than 0.5 ºC after stabilization, in Multi-Channel Temperature, a thermal image is taken using a Thermal Camera (Fluke Ti300) for a specific time.

All of the experimental tests were carried out at the Mechanical Engineering Department Laboratories in the College of Engineering at Al-Qadisiyah University.

2.8. Achieve device readings

To ensure that item was functioning appropriately, the thermocouple findings were compared to data gathered from thermal imaging. This includes Figure 6a depicts two scenarios for horizontal temperature distribution (i.e. x-axis) at the cavity center line, while Figure 6b. shows a comparison of the temperature distribution inside all the cavity (the thermocouples located in the middle, the top and bottom thirds of the cavity) and the thermal camera that measures the surface of the cavity.
The comparison revealed an excellent agreement between the experimental findings in all circumstances, which is an essential indicator of the practical part's correctness.

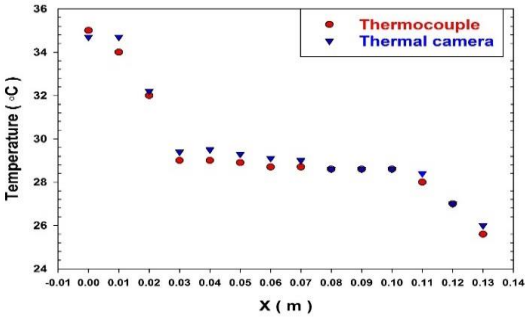

(a)

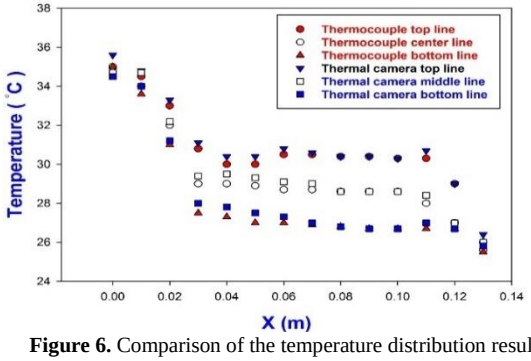

(b)

Figure 6. Comparison of the temperature distribution results from thermocouples and thermal camera at (a) at the enclosure's middle line, (b) at all positions of the enclosure (middle, top, and bottom line) for Hybrid nanofluid (θ = 0◦, Φ = 0.03%, ΔT= 10 ◦C).

3. Results and discussion

The outcomes of using the test rig to analyze natural convection heat transmittion are displayed. PCM will be added to the left side attached to the heated surface in the middle alone, and the top and lower cavities of the PCM cavity will be lodded with distilled Water. The right cavity will be packed with a hybrid nanofluid, and the impact of modifying the rest variables on the PCM and the hybrid nanofluid will be examined by using

a thermal imaging camera and thermocouples, and the temperature distribution within the cavity was obtained. A thermal camera and thermocouples.The experiments are included in one group in this section according to the PCM's location in the cavities linked to the hot wall and the following criteria:

1. The volume fraction of nanoparticles; Φ(0.03,0.05 , 0.07%).
2. Inclination angle of enclosure; θ (0◦,30◦,45◦).
3. The difference in temperature between the chilly and heated walls; ΔT (10, 15, and 20) ºC.
4. Times at (15, 30, and 60) min.

3.1. Effects of PCM and hybrid nanofluid

Fig.7 and Fig. 8 show temperature distribution over time with the whole PCM whenever concentration of hybrid nanofluid at θ =0◦, Φ=0.03 %, , ΔT=10,15, and 20 ºC. Where the temperature of the warm surface is 35◦C (ΔT = 10), Solubility of PCM has not been observed even on arrival to a steady condition. Paraffin wax's high latent heat created this. A consistent decline rate for hot wall temperature has been recorded at 10 %; decline rate at ΔT = 15°C is 14% and the decline rate at ΔT = 20°C is 15%.

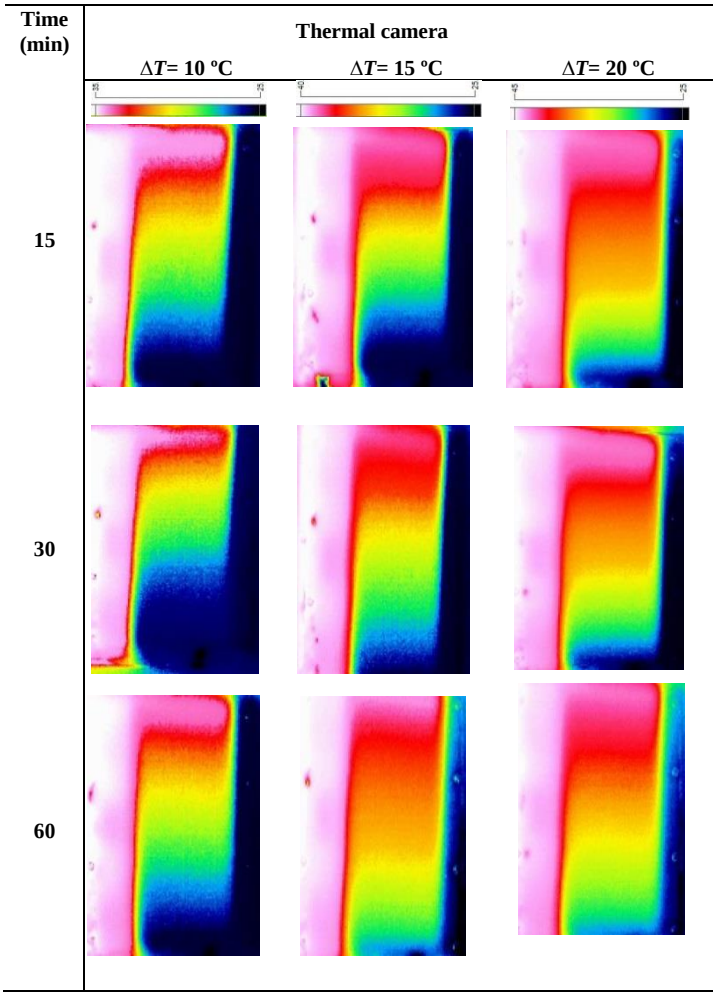

Figure 7. Temperature distribution in hybrid nanofluid and PCM enclosures at various times at θ = 0°, Φ = 0.03, , ΔT=10, 15 and 20 ºC.

Hybrid nanofluids' impact and because of the natural convection heat transmittion between the Water up and down the PCM material in the cavity will result in heat transfer through the water layer directly from the hot wall to the hybrid nanomaterial cavity accompanied by a small temperature reduction, the heat exchange area is also increased as a result of the PCM being surrounded with Water from up and down and thus accelerating the process of wax dissolution due to the small amount of paraffin wax, and thus the warming of the nanofluidic cavity, which appears to be evident in the chromatography.

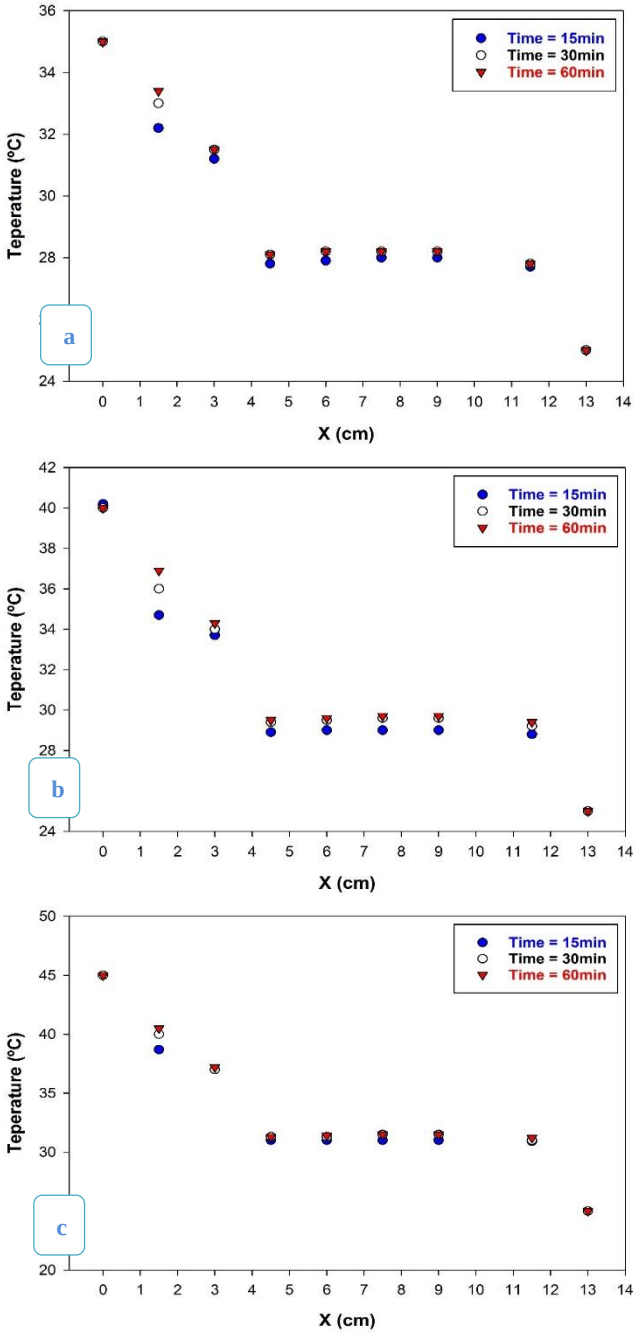

Figure 8. Temperature graphs at the enclosure's midline over time for PCM and hybrid nanofluid at Φ = 0.03, θ=0º, (a) at ΔT=10◦C; (b) at ΔT=15◦C; (c)at ΔT=20◦C.

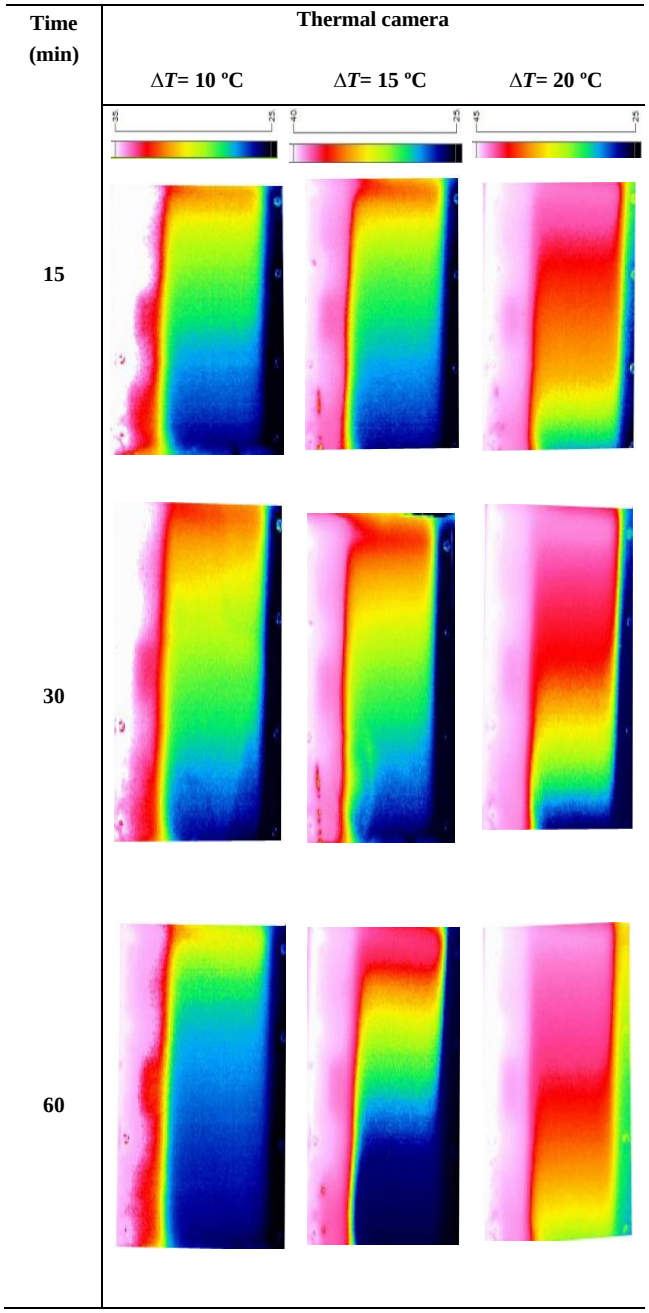

Figure 9. Temperature distribution in hybrid nanofluid and PCM enclosures at various times at θ = 0° , Φ = 0.05, , ΔT=10,15 and 20 °C.

3.2. Effects of PCM and hybrid nanofluid

Fig. 10 and Fig. 11 demonstrate the temporal dispersion of temperatures using full PCM whenever concentration of hybrid nanofluid φ = 0.05%, θ = 0◦, ΔT=10,15,20°C. The warm surface temperature is 35 ◦C (ΔT=10), and PCM's solubility has not been recorded even on arrival to a constant state. This was due to the high latent heat of paraffin wax. A consistent decline rate for hot wall temperature has been recorded at 11 %. The temperature of the PCM in the top cavity is higher than in the middle and bottom cavities, and the difference reaches 3 °C owing to natural convection currents in the hybrid nanofluids cavity generated by buoyancy force. After increasing the temperature of the hot surface to 40 C (ΔT = 15), it is clear that heat transmission by conduction is dominant, with a 15% pace at which the hot wall temperature drops.

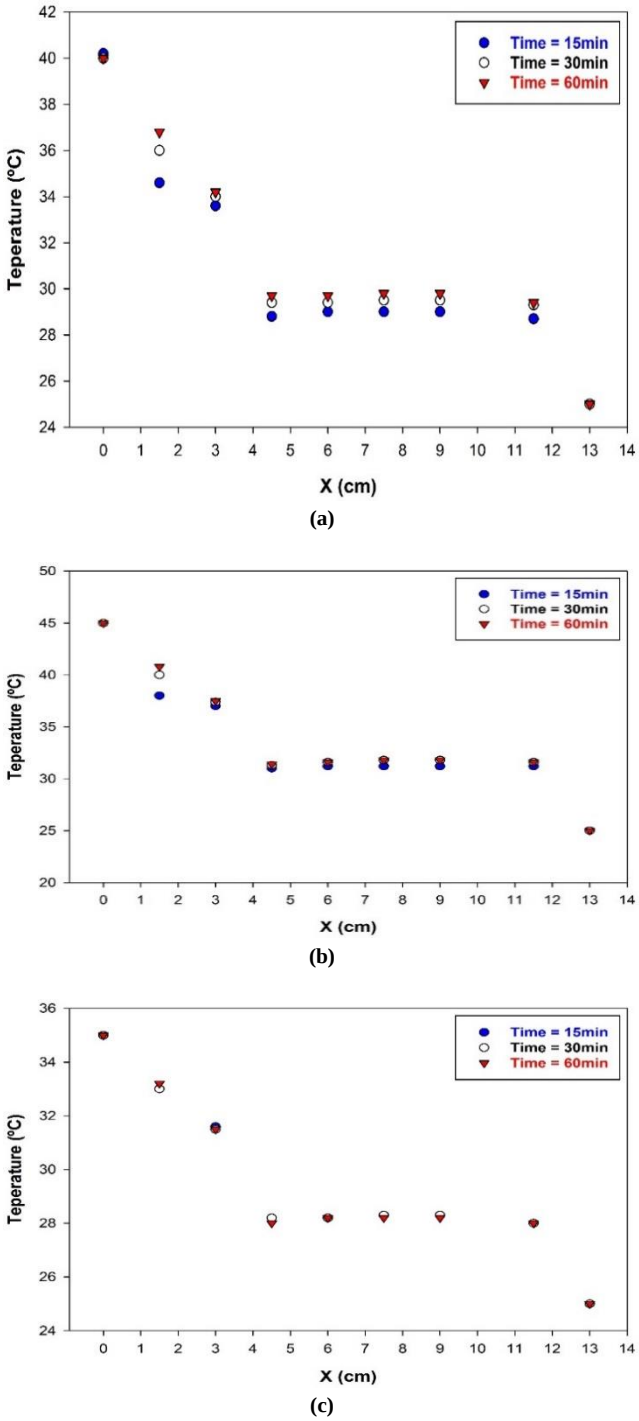

Figure 10. Temperature profiles at the enclosures' midpoints at (a) ΔT=10◦C; (b) ΔT=15◦C; (c) ΔT=20◦C.

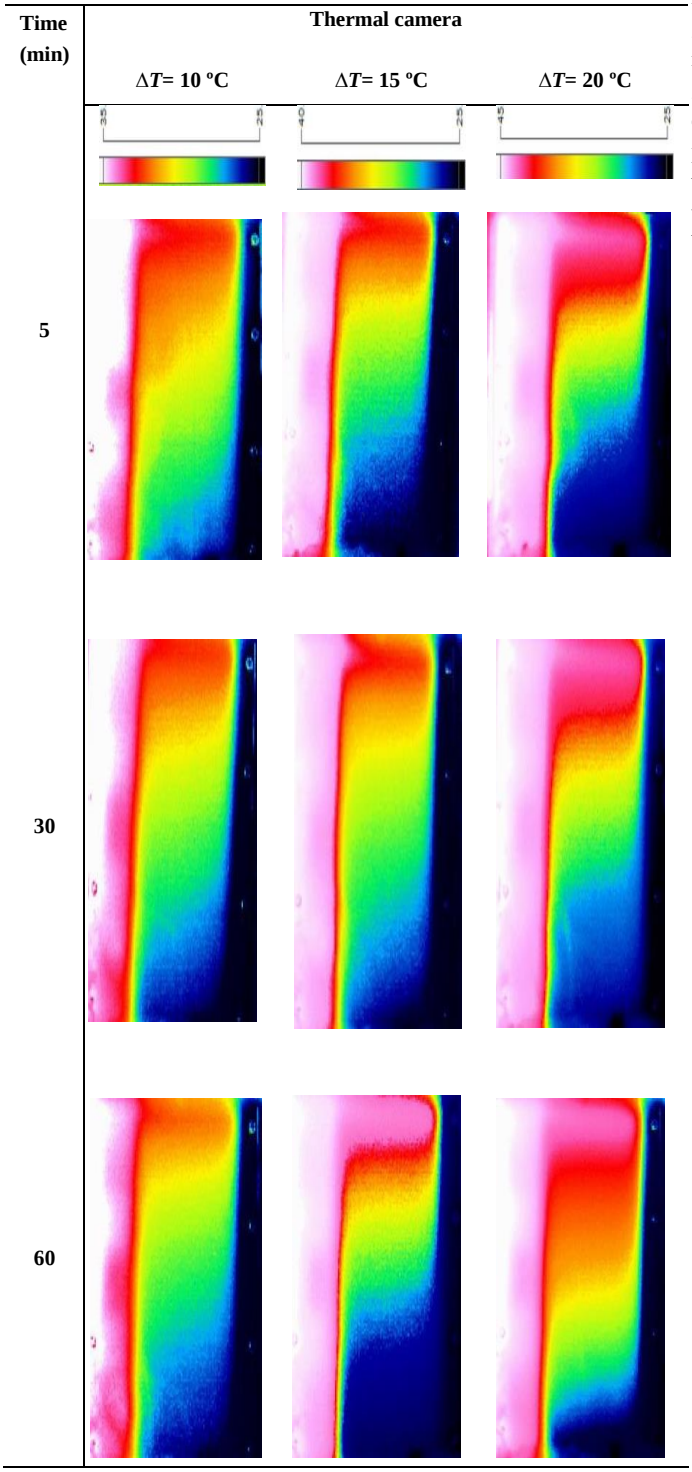

Figure 11. Temperature distribution in hybrid nanofluid and PCM enclosures at various times at θ = 0º , Φ = 0.07, , ΔT=10,15 and 20 ºC.

Near the left surface's, the temperature reaches 45°C (ΔT = 20). Particularly at the top of the enclosure, the paraffin wax becomes relatively liquid. Free convection dominates heat transfer, having the highest temperature on the PCM's upper left side enclosure as well as the coldest temperature on the lower left side of the moreover enclosure full of a hybrid nanofluid. In this instance. The rate of reduction in hot wall temperature was 15.5%. In general, whenever the hot wall temperature rises (over 38°C), the melting rate of paraffin wax increases; even though the hot wall temperature is greater than or equal to the melting point temperature of paraffin wax, it does not reach the entire melting stage. This is because the hybrid nanofluid promotes heat transport (heat removal) via natural convection, allowing the wall adherent to the PCM chamber's right wall to remain chilly. Also, as time passes, the effect of heat transmittion by free convection due to buoyancy force is seen in the hybrid nanofluid enclosure.

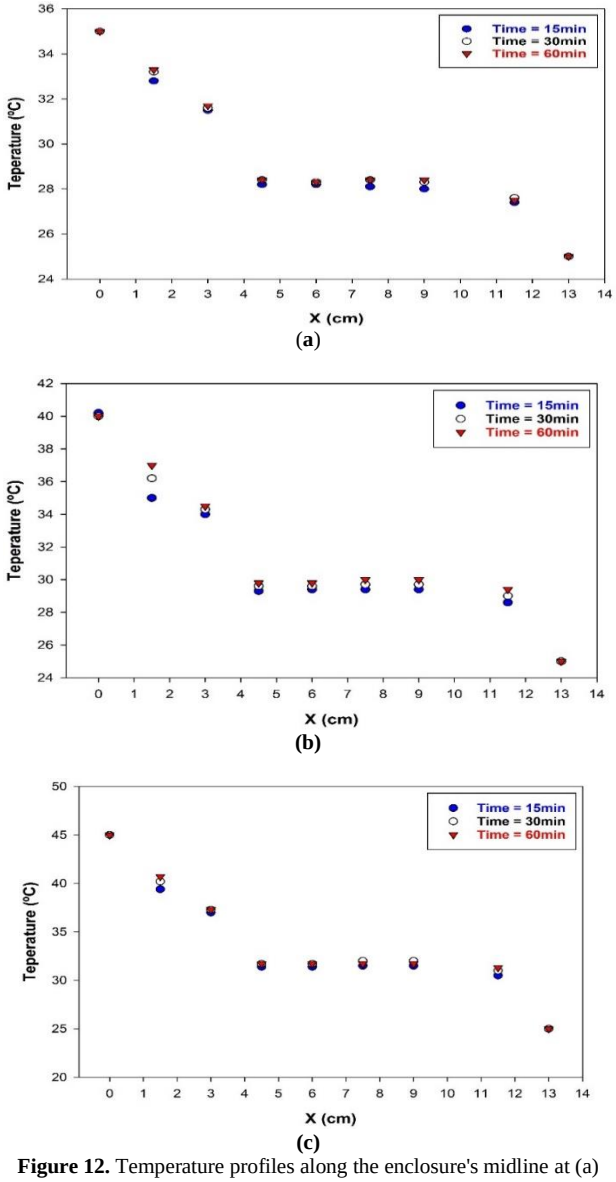

Figure 12. Temperature profiles along the enclosure's midline at (a) ΔT=10°C; (b) ΔT=15°C; (c) ΔT=20°C.

When the quantity of heat evacuated is increases, the temperature inside the enclosure decreases. This is evidenced by the increased heat transfer rate and temperature decrease of PCM, which accelerates the heated wall's cooling process. Fig. 12 and Fig. 13 demonstrate the temperature profile overtime whenerver a hybrid nanofluid at $\Phi = 0.07\%, \theta = 0°,$ and $\Delta T = 10, 15, 20$ C°

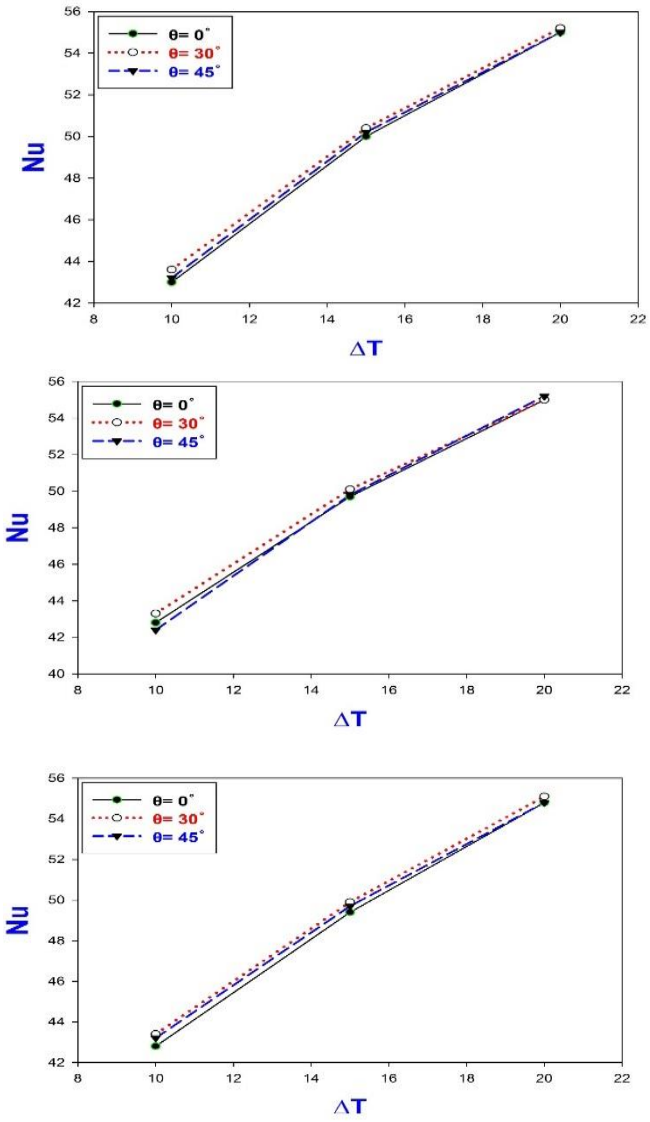

Figure 13. temperature profile over time whenever a hybrid nanofluid at Φ = 0.07%, θ = 0◦, ΔT=10,15,20 ºC.

Where the temperature difference is *(*ΔT = 10*)*, heat conduction is the major mode as a result of The paraffin wax does not remain firm. In the paraffin wax cavity, the decrease rate is 10.5%. A lowered rate of 14% was reported whenever hot surface temperature was 40°C (ΔT = *15*). The hot wall temperature hit 45 °C, The paraffin wax melted, causing temperature to drop 15.5%. Fig. 14 presents the impact of hybrid nanofluid volume fraction on Nusselt number with temperature differentials at different inclination angles. The Nusselt number increases by increasing concentration of the hybrid nanofluid and temperature gradient. This is due to the presence of PCM in the middle cavity only, while the other two parts fill the cavity attached to the hot wall with water. Due to the high thermal conductivity of Water compared with PCM, a large amount of heat quickly travels to the hybrid nanofluid cavity. Moreover, because using PCM along the hot wall lowers the temperature of the hot surface due to its high latent heat, the quantity of heat transmitted from the hot wall to the hybrid nanofluid is augmented.

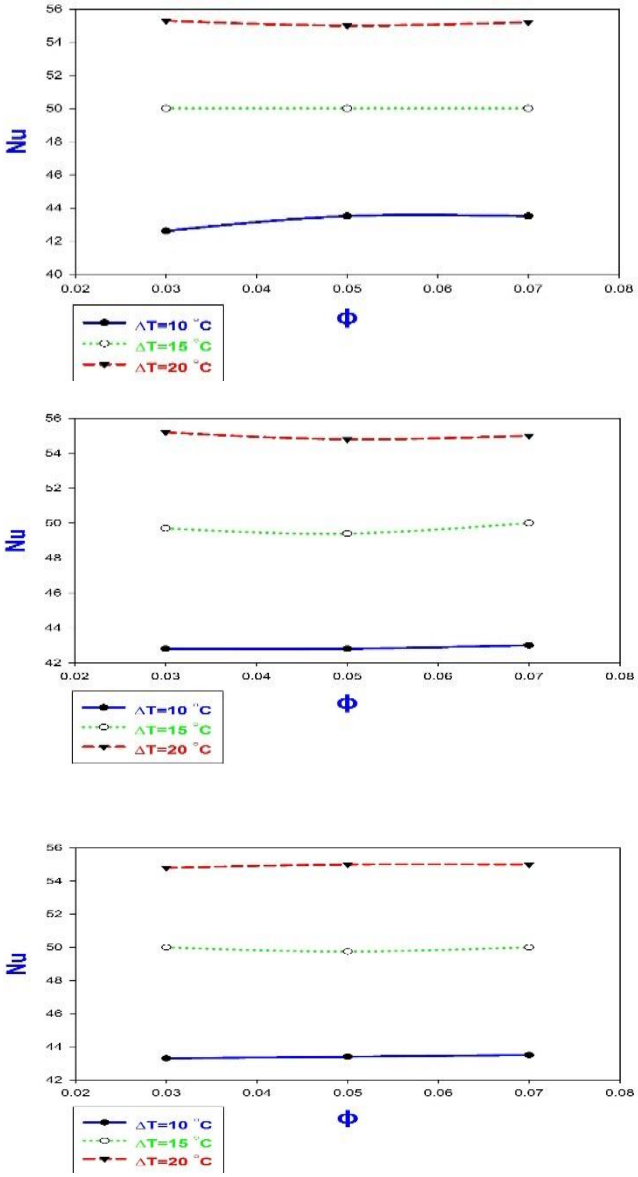

Fig. 14. shows the impact of temperature differentials on the Nusselt number and cavity inclinations, where the value of the Nusselt number increases with growing temperature differentials. Also, the highest value for the Nusselt number occurs at the inclination angle θ = 30◦.

4. Conclusions

The results can be summarized as follows:

1. Temperatures were discovered to be more evenly distributed in the cavity's upper half as a result of buoyancy force and different densities due to Natural convection.
2. As the concentration of hybrid nanofluid grows, so does its thermal conductivity; as a result of the high conductivity of heat of hybrid nanomaterial, the decreased rate of heat transmission increases.
3. Where proportionality is created between hot and cold walls, the temperature differential impacts the decrease rate, with the largest value

when the difference is $\Delta T = 20^{\circ}C$ and reaches 15.5 %.

4. Increasing the number of Nusselt means increasing the natural convection heat transmission rate during the nanofluid enclosure. However, it also shows that a significant quantity of heat passed via the center wall due to the absence of paraffin wax, which is responsible for decreasing the temperature.
5. The Nusselt number rises as nanomaterial concentration rises, owing to enhanced heat interaction between the hybrid nanofluid and paraffin wax. As we formerly showed by raising the concentration of hybrid nanofluids, heat transmission by free convection increases as the conductivity of heat increases.

Authors' contribution

All authors contributed equally to the preparation of this article.

Declaration of competing interest

The authors declare no conflicts of interest.

REFERENCES

[1] M.S. Sadeghi, N. Anadalibkhah, R. Ghasemiasl, T. Armaghani, A.S. Dogonchi, A.J. Chamkha, H. Ali, A. Asadi, On the natural convection of nanofluids in diverse shapes of enclosures: an exhaustive review, Journal of Thermal Analysis and Calorimetry, (2020) 1-22.

[2] I. Garbadeen, M. Sharifpur, J. Slabber, J. Meyer, Experimental study on natural convection of MWCNT-water nanofluids in a square enclosure, International Communications in Heat and Mass Transfer, 88 (2017) 1-8.

[3] R. Mohebbi, S.H. Khalilabad, Y. Ma, Effect of γ -Al2O3/Water Nanofluid on Natural Convection Heat Transfer of Corrugated¬ Shaped Cavity: Study the Different Aspect Ratio of Grooves, Journal of Applied Fluid Mechanics, 12(4) (2019) 1151-1160.

[4] A.D. Abdulsahib, K. Al-Farhany, Review of the Effects of Stationary/Rotating Cylinder in a Cavity on the Convection Heat Transfer in Porous Media with/without Nanofluid, Mathematical Modelling of Engineering Problems, 8(3) (2021) 356-364.

[5] K.K. Al-Chlaihawi, H.H. Alaydamee, A.E. Faisal, K. Al-Farhany, M.A. Alomari, Newtonian and non-Newtonian nanofluids with entropy generation in conjugate natural convection of hybrid nanofluid-porous enclosures: A review, Heat Transfer, 51(2) (2022) 1725-1745.

[6] T. Tayebi, H.F. Öztop, A.J. Chamkha, Natural convection and entropy production in hybrid nanofluid filled-annular elliptical cavity with internal heat generation or absorption, Thermal Science and Engineering Progress, 19 (2020) 100605.

[7] B.M. Amine, F. Redouane, L. Mourad, W. Jamshed, M.R. Eid, W. Al-Kouz, Magnetohydrodynamics Natural Convection of a Triangular Cavity Involving Ag-MgO/Water Hybrid Nanofluid and Provided with Rotating Circular Barrier and a Quarter Circular Porous Medium at its Right-Angled Corner, Arabian Journal for Science and Engineering, 46(12) (2021) 12573-12597.

[8] C. Revnic, T. Groşan, M. Sheremet, I. Pop, Numerical simulation of MHD natural convection flow in a wavy cavity filled by a hybrid Cu-Al 2 O 3-water nanofluid with discrete heating, Applied Mathematics and Mechanics, 41(9) (2020) 1345-1358.

[9] A.J. Chamkha, I.V. Miroshnichenko, M.A. Sheremet, Numerical analysis of unsteady conjugate natural convection of hybrid water-based nanofluid in a semicircular cavity, Journal of Thermal Science and Engineering Applications, 9(4) (2017) 041004.

[10] M.A. Alomari, K. Al-Farhany, A.L. Hashem, M.F. Al-Dawody, F. Redouane, O.A. Olayemi, Numerical study of mhd natural convection in trapezoidal enclosure filled with (50%mgo-50%ag/water) hybrid nanofluid: Heated sinusoidal from below, International Journal of Heat and Technology, 39(4) (2021) 1271-1279.

[11] F. Redouane, W. Jamshed, S.S.U. Devi, B.M. Amine, R. Safdar, K. Al-Farhany, M.R. Eid, K.S. Nisar, A.H. Abdel-Aty, I.S. Yahia, Influence of entropy on Brinkman–Forchheimer model of MHD hybrid nanofluid flowing in enclosure containing rotating cylinder and undulating porous stratum, Scientific Reports, 11(1) (2021).

[12] M. Kheradmand, M. Abdollahzadeh, M. Azenha, J. de Aguiar, Phase change materials as smart nanomaterials for thermal energy storage in buildings, Intelligent Nanomaterials, 2 (2016) 247-293.

[13] Y. Hong, W.-B. Ye, J. Du, S.-M. Huang, Solid-liquid phase-change thermal storage and release behaviors in a rectangular cavity under the impacts of mushy region and low gravity, International Journal of Heat and Mass Transfer, 130 (2019) 1120-1132.

[14] M. Parsazadeh, M. Malik, X. Duan, A. McDonald, Numerical study on melting of phase change material in an enclosure subject to Neumann boundary condition in the presence of Rayleigh-Bénard convection, International Journal of Heat and Mass Transfer, 171 (2021) 121103.

[15] A. Labihi, F. Aitlahbib, H. Chehouani, B. Benhamou, M. Ouikhalfan, C. Croitoru, I. Nastase, Effect of phase change material wall on natural convection heat transfer inside an air filled enclosure, Applied Thermal Engineering, 126 (2017) 305-314.

[16] T. Bouhal, O. Limouri, Y. Agrouaz, T. Kousksou, Y. Zeraouli, A. Jamil, Numerical analysis of PCM melting filling a rectangular cavity with horizontal partial fins, in: MATEC Web of Conferences, EDP Sciences, 2020, pp. 01011.

[17] A. Chamkha, A. Doostanidezfuli, E. Izadpanahi, M. Ghalambaz, Phase-change heat transfer of single/hybrid nanoparticles-enhanced phase-change materials over a heated horizontal cylinder confined in a square cavity, Advanced Powder Technology, 28(2) (2017) 385-397.

[18] A. Laouer, K. Al-Farhany, M.F. Al-Dawody, A.L. Hashem, A numerical study of phase change material melting enhancement in a horizontal rectangular enclosure with vertical triple fins, International Communications in Heat and Mass Transfer, 137 (2022).

[19] A. Laouer, K. Al-Farhany, Melting of nano-enhanced phase change material in a cavity heated sinusoidal from below: Numerical study using lattice Boltzmann method, Heat Transfer, 51(6) (2022) 5952-5970.

[20] H. Shili, K. Fahem, S. Harmand, S. Ben Jabrallah, Thermal control of electronic components using a liquid around the phase change material, Journal of Thermal Analysis and Calorimetry, 140(3) (2020) 1177-1189.

[21] T.H. Kean, N.A.C. Sidik, J. Kaur, Numerical investigation on melting of Phase Change Material (PCM) dispersed with various nanoparticles inside a square enclosure, in: IOP Conference Series: Materials Science and Engineering, IOP Publishing, 2019, pp. 012034.

[22] M. Sivashankar, C. Selvam, S. Manikandan, S. Harish, Performance improvement in concentrated photovoltaics using nano-enhanced phase change material with graphene nanoplatelets, Energy, 208 (2020) 118408.

[23] S. Ebadi, S.H. Tasnim, A.A. Aliabadi, S. Mahmud, Melting of nano-PCM inside a cylindrical thermal energy storage system: Numerical study with experimental verification, Energy Conversion and Management, 166 (2018) 241-259.

[24] A. Abdelrazik, F. Al-Sulaiman, R. Saidur, Numerical investigation of the effects of the nano-enhanced phase change materials on the thermal and electrical performance of hybrid PV/thermal systems, Energy Conversion and Management, 205 (2020) 112449.

[25] S. Nada, D. El-Nagar, H. Hussein, Improving the thermal regulation and efficiency enhancement of PCM-Integrated PV modules using nano particles, Energy conversion and management, 166 (2018) 735-743.

[26] S. Chavan, D.A. Perumal, V. Gumtapure, Numerical Studies For Charging And Discharging Characteristics Of Composite Phase Change Material In A Deep And Shallow Rectangular Enclosure, in: IOP Conference Series: Materials Science and Engineering, IOP Publishing, 2018, pp. 012059.

[27] F. Asdrubali, F. D'Alessandro, S. Schiavoni, A review of unconventional sustainable building insulation materials, Sustainable Materials and Technologies, 4 (2015) 1-17.

[28] K.H. Hilal Fluid Flow and Heat Transfer Characteristics in a Vertical Tube Packed Bed Media, University of Technology, (2004).

[29] A. Moradi, M. Zareh, M. Afrand, M. Khayat, Effects of temperature and volume concentration on thermal conductivity of TiO2-MWCNTs (70-30)/EG-water hybrid nano-fluid, Powder Technology, 362 (2020) 578-585.

[30] B. Rahmatinejad, M. Abbasgholipour, B. Mohammadi Alasti, Investigating thermo-physical properties and thermal performance of Al2O3 and CuO nanoparticles in Water and Ethylene Glycol based fluids, International Journal of Nano Dimension, 12(3) (2021) 252-271.

[31] B.C. Pak, Y.I. Cho, Hydrodynamic and heat transfer study of dispersed fluids with submicron metallic oxide particles, Experimental Heat Transfer an International Journal, 11(2) (1998) 151-170.

[32] M. Mansour, S. Siddiqa, R.S.R. Gorla, A. Rashad, Effects of heat source and sink on entropy generation and MHD natural convection of Al2O3-Cu/water hybrid nanofluid filled with square porous cavity, Thermal Science and Engineering Progress, 6 (2018) 57-71.